

Fiber Optic Strain Gage Verification and Polyethylene Hip Liner Testing

Lucas Chavez¹, Michael Martin², Stephen O. Neidig³, Phillip Cornwell⁴, R. Michael Meneghini⁵, Joe Racanelli⁶

¹ New Mexico Institute of Mining and Technology, Socorro, NM, 87801

² Texas A&M University, College Station, TX, 77840

³ University of New Mexico, Albuquerque, NM, 87106

⁴ Rose-Hulman Institute of Technology, Terre Haute, IN 47803

⁵ New England Musculoskeletal Institute, University of Connecticut Health Center, Farmington, CT 06030

⁶ Stryker Orthopaedics, Mahwah, NJ 07430

Abstract

To optimize stability in total hip arthroplasty, the use of larger femoral heads necessitates a polyethylene liner of reduced thickness. An understanding of the mechanical properties, particularly resistance to fatigue failure, of highly-crosslinked polyethylene is critical to determine the optimal parameters for clinical use. The primary purposes of this study were to characterize the X3™ highly cross-linked polyethylene (HCLPE) liner peripheral face strain field in multiple orthopaedic acetabular shell constructs under physiological loading and to evaluate the usefulness of fiber optic strain gages in this type of biomedical application. The first phase of this study involved measuring X3 HCLPE material properties in tension and compression using uniaxial fiber optic strain gages and resistance based uniaxial and multi-axial (rosette) strain gages to gain greater insight into the complexities and limitations of the use of fiber optic strain gages with X3 HCLPE. In the second phase, physical testing was used to evaluate the effect of HCLPE thickness on the hoop strain field of liner samples of three different thicknesses at three inclination angles and three head offsets that simulate potential in vivo clinical scenarios occurring in hip replacement. The results from these studies will be presented in this paper.

1 Introduction

1.1 Background

Statistics show that between 200,000 and 300,000 total hip replacements occur every year in the United States [1]. With such a large number of people receiving hip replacements, ensuring that these devices function properly is extremely important. One study of hip replacement reliability found that 3.9% of total hip replacement patients dislocated within the first 6 months after surgery and 30% dislocated after 5 years [2]. Several factors contributed to these problems including femoral component head size, acetabular component orientation, and excessive wear of the acetabular polyethylene liner which has been linked to osteolysis [3]. These components must be designed appropriately to withstand such problems in a hostile and dynamic environment. It has been shown that during normal-level walking the hip joint can encounter resultant forces from five to eight times the body weight of the individual [4]. During the swing phase of normal level walking, the femoral head and acetabular component have been shown to separate up to 2.8 mm [3]. This dislocation can result in less than optimal head/liner contact leading to edge loading the rim of the acetabular liner. This loading condition may lead to increase strain in the liner rim and increased wear.

1.2 Motivation

Studies have been conducted to investigate the dislocation issue, and one potential solution is to increase the size of the femoral head [2]. Results indicated that increasing the femoral head diameter has a two-fold advantage. First, an increased femoral head size increases the vertical femoral head displacement

(VHD) that the head must experience before dislocation can occur. As shown in Crowninshield et al., the VHD increases from 3.2 to 5.8 mm when the head size is increased from 22 to 40 mm with an acetabular component oriented at 45°. Also, when the head size changes from 22 to 44 mm, the prosthetic impingement free range of motion (PIF-ROM) is increased by approximately 30°. However, coupled with these two advantages is an obvious constraint problem, that is, with increased head size and fixed acetabular component size, the liner cup thickness must decrease. Therefore, the threat of liner wear becomes an even more prevalent problem in hip replacement [2].

Hip liners are traditionally made from ultra high molecular weight polyethylene (UHMWPE). This particular polymer has outstanding mechanical properties and has been used in orthopedics as a load bearing material in artificial joints for the last 40 years. The leading factor limiting the longevity of implants made from UHMWPE is wear [5]. The wear properties of the material can be increased by cross-linking through exposure to gamma sterilization. Stryker uses a number of PE materials for hip liners including N2Vac which are machined from compression molded GUR 1020 bar stock, packaged in nitrogen and sterilized using 30 kGy gamma irradiation and is packaged in a nitrogen environment to prevent oxidation. [6]

A potential solution to the problem of creating thinner liners with sufficient wear performance is the use of highly cross-linked polyethylene materials. One such material is Polyethylene X3™. This material is manufactured by Stryker from a compression molded GUR 1020 sheet which is sliced into rectangular bars. These bars are further processed to received 30 kGy gamma irradiation (Co60 source) followed by an annealing step at 130 °C for 8 hours. This process is performed three times to accumulate a total dose of 90 kGy in these bars. Experiments have shown that this material has a 97% lower wear rate than conventional polyethylene. In addition, this material maintains a high resistance to oxidation — a critical property for material survival in the human body — as well as good mechanical performance over time [7]. Liners with minimum radial thicknesses of four mm have been manufactured using this new material.

It is difficult to measure the strains in thin liners or on the thin liner face with conventional methods such as resistance based strain gauges. These transducers are far too large to measure the peripheral strain field on the line face.. Fiber optic strain gauges, however, are extremely narrow. Some are only 0.23 mm in diameter, making them prime candidates for monitoring the strain field of a liner under load [8-12]. Due to their geometry, fiber optic strain gauges can be used in situations where bulkier, larger resistance strain gages are not feasible. Furthermore, they are inert to any type of electromagnetic interference. Fiber optic strain gages can also be integrated into structures such as composite materials, allowing for the measurement of internal strains.

The fiber optic strain gages investigated in this study use Bragg Gratings. A Bragg Grating is a “periodic perturbation of the refractive index which is laterally exposed in the core of an optical fiber,” [13] where the refractive index is defined as the ratio of the velocity of light in a vacuum to that in a medium. The grating determines what wavelengths of the incoming light wave are reflected. When this grating is stretched due to a mechanical strain, the grating spacing changes and therefore a different wavelength is reflected. This change can be directly related to the strain of the fiber.

1.3 Purpose

The purposes of this study were to characterize the X3™ highly cross-linked polyethylene (HCLPE) liner peripheral face strain field in multiple orthopaedic acetabular shell constructs under physiological loading and to evaluate the usefulness of fiber optic strain gages in this type of biomedical application. The first phase of this study was to determine X3 HCLPE material properties, such as elastic modulus and Poisson's ratio, in tension and compression using uniaxial fiber optic strain gages and resistance based uniaxial and multi-axial (rosette) strain gages. Multiple tension and compression specimens were tested using ASTM standards to determine these properties. The strain in the specimens was monitored using standard resistance based strain gages, fiber optic strain gages, and an extensometer. By comparing the three sets of strain data, the validity of the fiber optic strain gage results was determined. Another goal of these tests was to provide insights into the complexities and limitations of the use of fiber optic strain gages with X3 HCLPE.

In the second phase, physical testing was used to evaluate the effect of HCLPE linear radial thickness on the hoop strain field of liner samples of three different thicknesses at three inclination angles and three head offsets that simulate potential in vivo clinical scenarios occurring in hip replacement. Liners made from N2Vac and X3 were tested. The peripheral face strain field for each test configuration was monitored using one or two fiber optic strain gages.

2 Experimental Procedure

2.1 Strain Gage and Polyethylene Considerations

2.1.1 Adhesion of Gages

Polyethylene is a difficult material to adhere to primarily due to its low surface tension. In order to properly adhere to polyethylene, the adhesive needs to have a lower surface tension than the polyethylene [14]. When this occurs, the adhesive has proper wetting. Figure 1 shows how proper wetting creates more surface area for adhesion. In an attempt to find a suitable adhesive for X3 HCLPE, different types of adhesive and surface preparations were investigated.

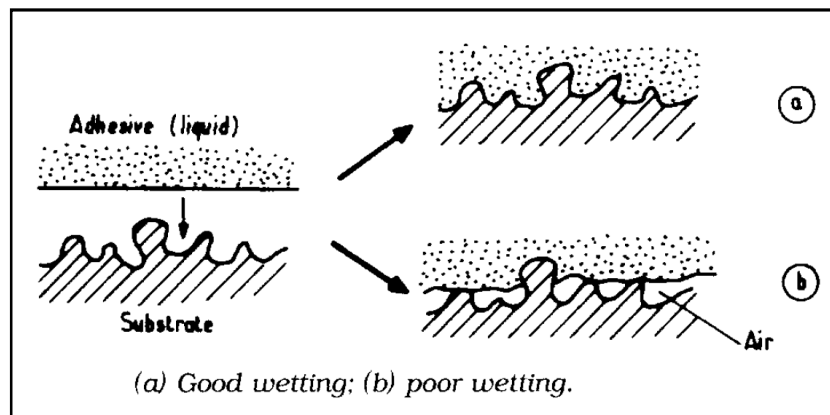


Figure 1: Diagram of proper wetting [8]

The first adhesive that was tried was M-Bond 200. This adhesive is commonly used for attaching strain gages, but when used in this application, resulted in very poor adhesion between the strain gages and the X3 HCLPE. This was evident in the stress-strain plot obtained in preliminary testing. The strain measured by the resistance and fiber optic strain gages deviated greatly from the strain measured by the extensometer. The second adhesive tried was Master Bond X17. Although this resulted in what appeared to be a good bond between the gages and the X3 HCLPE, the first tensile test also resulted in very poor correlation between the strain gages and the extensometer results. It was later determined that the shear strength of the epoxy was much too small for adequate strain transfer. Various surface preparations were also tried including Master Bond X17 as a primer with an epoxy as the adhesive, but with no improvement in the adhesion. The next adhesive tried was Barco Bond epoxy, because it has a high shear strength. With Barco Bond epoxy, it was difficult to smooth the epoxy out from underneath the gage, so the gage was measuring the strain in the epoxy and not in the polyethylene [15]. Finally, an adequate epoxy was found called Bondit B-481 TH. Bondit B-481 TH is a two part epoxy with a high modulus of elasticity compared to the polyethylene. This relatively high modulus transfers the strain from the specimen to the gage. In addition, this adhesive has a relatively low surface tension compared to the M-bond 200 and other epoxies. It also is viscous enough to smooth a thin layer of the adhesive under the gage.

2.1.2 Strain Gage Application

To apply the resistance strain gages, the surface of the sample was sanded in two directions 90° apart to form cross hatching. After the surface was sanded, it was cleaned and degreased using methanol and

Kimwipes. Gage tape was used in the conventional manner to stick the gage to the tape and orient it on the specimen. The tape was then peeled back to expose the underside of the gage for cleaning. Then, Bondit was applied to the gage. The tape was smoothed back onto the sample by pressing on it with a finger, keeping the gage from moving.

To attach the fiber optic strain gage the surface was prepared in the same fashion as the resistance gages. The gage length was located by looking at the wavelength and applying a pressure across the manufacture specified length of the fiber optic. Once located, it was marked and laid across the desired section of the specimen and the ends were taped to the specimen. The gage length was then adhered to the sample using the Bondit.

2.2 Specimen Testing

2.2.1 Tensile Test

The first test to be performed was a standard tensile test that was performed in accordance with ASTM D638-08 using a Type I sample with dimensions 6.35 mm (0.25 in.) thick and 165 mm (6.5 in.) long [16]. A specimen in the Instron grips is shown in Figure 2. The tests were run at 2.0 mm/min (0.079 in./min) and at room temperature. This load rate is slower than the ASTM standard in order to obtain more data points. The samples were instrumented with a fiber optic gage mounted longitudinally on one face of each sample and one resistance based rosette strain gage mounted on the opposite side of the same sample. The gages were mounted as close as possible to the middle of each specimen. An extensometer was then attached to the sample. A 5 kN load cell was used to measure the force. The samples were loaded to approximately 4% strain according to the extensometer. Good data from three samples were obtained. More samples were tested, but problems associated with adhering the gages resulted in bad data.



Figure 2: Tension test sample in Instron test machine

2.2.2 Compression Test

The second test to be performed was a compression test that was done in accordance with ASTM D695-08. A 25.4 mm (1.0 in.) diameter, 63.5 mm (2.5 in.) long cylindrical sample was used to minimize the barreling effect [17]. A photo of an instrumented sample is shown in Figure 3. In this figure the strain gage rosette and extensometer are pictured. The test was run at 2.0 mm per minute (0.079 in./min) and at room temperature.

One longitudinal fiber optic gage and a resistance strain gage rosette were mounted on each sample 180° apart about the circumference of the cylinder. The gages were mounted as centrally as possible along the longitudinal axis of the cylinder. The compression fixture as shown in Figure 3 was mounted into the Instron testing machine. The longitudinal strain was measured from the fiber optic gage and the longitudinal and transverse strains were measured using the rosette. Good data from three samples were obtained.

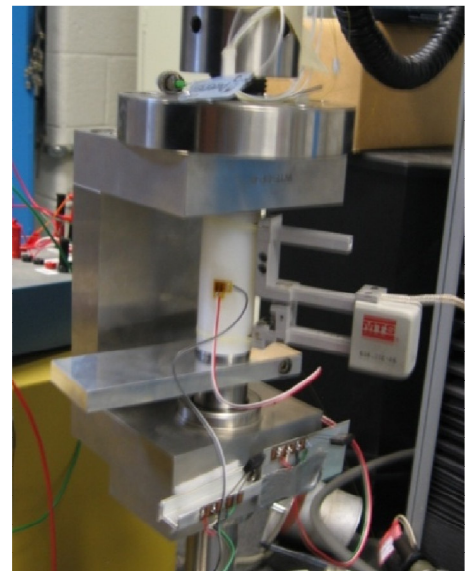


Figure 3: Instrumented compression sample

2.3 Clinical Testing

The second aspect of this study was to investigate the hoop strain of various X3 HCLPE liners and to compare these results to finite element results. The liners were inserted into titanium acetabular shells

that were in potted aluminum fixtures. A test matrix of the tests to be performed is shown in Table 1. A total of nine measurements were taken for each liner size, corresponding to three offsets for each inclination angle. In Table 1 N2Vac refers to Stryker’s nitrogen treated polyethylene.

Table 1: Test matrix for clinical testing

Liner Material	Liner Diameter (mm)	Inclination Angle (Degrees)	Separation Offset (mm)
X3 HCLPE	36	45,55,65	0,1,2
X3 HCLPE	40	45,55,65	0,1,2
X3 HCLPE	44	45,55,65	0,1,2
N2Vac	44	45,55,65	0,1,2

Once the liner was in the shell, fiber optic strain gages were mounted on the top surface lip of the liner. The fiber optic strain gage was placed in the middle of the thickness of the lip of the liner as shown in Figure 4. The area was sanded and the gage was placed using similar mounting techniques as was used on the tension and compression samples. On the 44 mm and 40 mm liners only one gage was used. On the 36 mm liners two gages were used. The thickness of the lip was separated into thirds and the gages were attached. Bondit was used in the application of all of the gages.

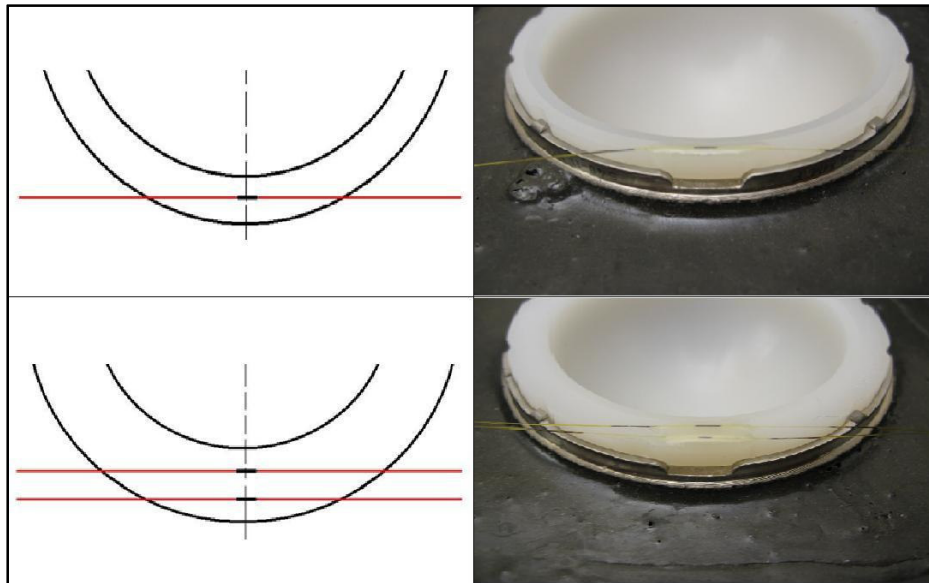


Figure 4: Gage locations for the 36 mm liner (bottom) and the 40 mm and 44 mm liners (top)

A Cobal Chrome plated stainless steel femoral head was mounted into a 5 kN load cell. A 2450 N force was applied to the liner and maintained for 30 seconds. The liner in the acetabular fixture was held by a movable vice as shown in Figure 5. This vice was used to alter the inclination angle of the mold as well as the offset distance from the load line. The offset was created by placing one or two 1.06 mm thick aluminum pieces between the vice and the aluminum holders. The hoop strain results from testing the X3 HCLPE liners were compared to the results from shells made of Stryker’s conventional polyethylene liner material, N2Vac.

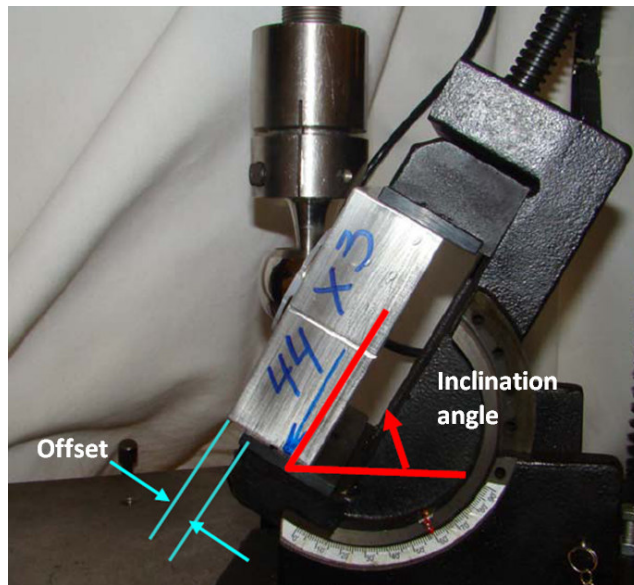


Figure 5: Test fixture used to hold the acetabular liners showing the offset and angle of inclination

During hip liner testing the compressive load was applied using a displacement of 5 mm/min. According to ASTM Standard D638-08, the speed is to be chosen so that rupture of the specimen occurs within 0.5 to 5 minutes. This standard lists several speeds for particular geometries, and based upon this test's geometry an estimation was made for the appropriate loading speed for the liner. Shown in Figure 6 is a typical loading curve for the liner, where the peak value is approximately 2450 N.

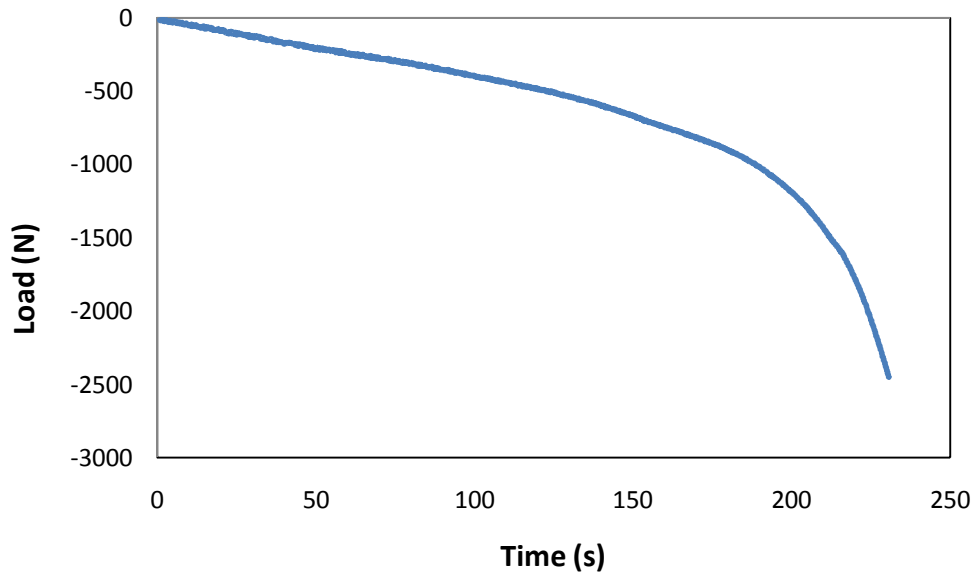


Figure 6: Typical loading curve for clinical liner testing

2.4 Data Acquisition

Two data acquisition systems were used in this study. One system used a LabVIEW VI to record wavelength measurements from the fiber optic gages as well as the time stamp of each sample. The front panel is shown in Figure 7. This system tracked the peak reflection wavelength transmitted by the fiber.

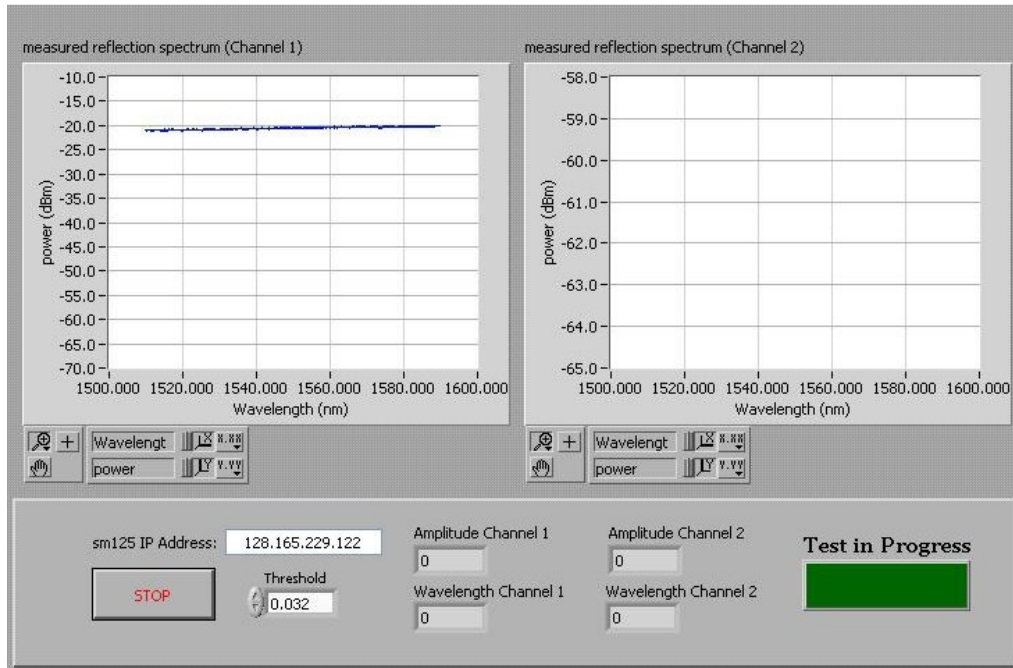


Figure 7: LabVIEW VI used to collect fiber optic gage readings

The second system acquired voltage readings from the resistive strain gages bridge circuit, load readings from the tensile machine, and strain measurements from the extensometer. Time stamps were recorded for each sample. For the subsequent analysis, the time signatures between the two systems needed to be aligned so that meaningful comparisons could be made. The LabVIEW program used to monitor the fiber optic gages was triggered at a specific load reading, either 25 N for the tensile tests or 100 N for the compression tests. A datum was established at this trigger point, and the time signature recorded by the other system at the trigger load was added to this datum. By doing this, all data was converted to the tensile machine time reckoning.

2.5 Calculations

To obtain useful data, the wavelength and voltage readings of the two types of strain gages needed to be converted to actual strain. To convert the wavelength readings into strain, the equation is

$$\varepsilon_F = \frac{\Delta\lambda}{(\lambda)(0.78)} \quad (1)$$

where λ is the wavelength recorded at the trigger point, $\Delta\lambda$ is the deviation from this datum wavelength, and 0.78 is the photo-elastic constant. The datum wavelength varied slightly from test to test, depending on numerous factors including the manufacture and possibly pre-stress on the fibers. The conversion equation for the resistance gages is

$$\varepsilon_R = V_R \frac{.0295}{8} \quad (2)$$

where V_R is the voltage output from the resistive strain gages, and the calibration constant is 2.95% strain for every 8 volts produced. Finally, the strain equation for the extensometer is

$$\varepsilon_E = \frac{\Delta L}{G_L} \quad (3)$$

where ΔL is the deviation from the datum length of the extensometer, G_L . Once these strain values were determined, the corresponding stress values needed to be matched. This was not difficult for the resistance gages or extensometer, as the same data acquisition system was used to sample these and the load on the specimen. For the fiber optic readings, the converted time signatures as described above were used to match stress data as taken by the tensile machine with the strain data taken at the same time by the fibers. Stress values were calculated using the engineering, or nominal, stress definition

$$\sigma_n = \frac{F}{A} \quad (4)$$

where F and A are the load reading and nominal cross-sectional area of the specimen whose normal is parallel to the load line, respectively. Engineering stress and strain plots were generated from the data for each test. To determine a tangent modulus a second order polynomial fit was applied to the extensometer data from 0 to 0.2% strain. Using the equation for this polynomial, the tangent modulus was calculated at 0.02% strain.

Poisson's Ratio was also calculated using the data acquired from the axial and transverse resistance gages using

$$\nu = -\frac{\varepsilon_z}{\varepsilon_y} \quad (5)$$

where ε_z and ε_y are the nominal strain values in the transverse and axial directions, respectively. This ratio was calculated for every data point recorded. When the values seemed to reach a constant value, an overall average was calculated.

3 Finite Element Models

Finite element models of the acetabular component were constructed to obtain insight into the anticipated strain values to be obtained from the experiment. Models using linear and non-linear material models were constructed in ANSYS. A cross section of the femoral head, X3 HCLPE liner, and acetabular cup is shown in Figure 8. The model used a single plane of symmetry to reduce the size of the model and the femoral head was modeled as being hollow. The femoral head is shown in red and different loading conditions were considered by offsetting the head normal to the face of the liner. A 2 mm offset is shown in Figure 8. The hip liner is held by a titanium shell that, in a patient, would be attached to the pelvis. A 2450 N vertical downward force was applied to the femoral head to model the loading conditions used in the experiment. Previous physical testing of X3 HCLPE provided the necessary properties used in the models.

Figure 9 shows an example of typical strain field contours obtained from a finite element analysis. These results are for a 36 mm diameter cup with a 2 mm offset. Figure 9 shows the maximum principle strains. This figure shows that there is a larger strain around the point of the loading. The maximum principle strain for this run was 0.5%. Since the fiber optic gages were to be placed in the hoop direction directly below the point of loading, contour plots of the strain in this direction were also created. Figure 10 shows the strain in this direction. Thus, these values are what were expected to be seen in the experiment.

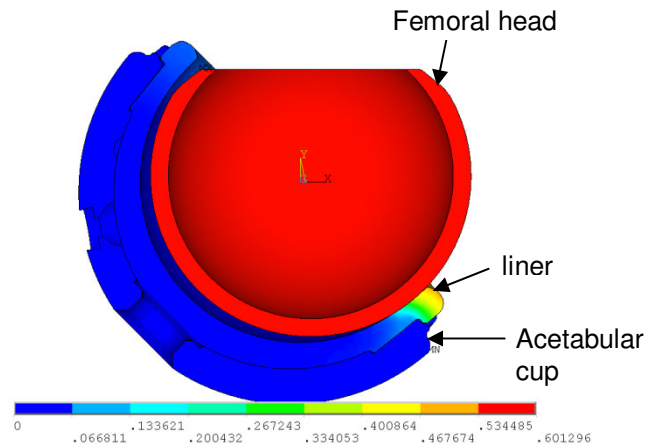


Figure 8: Cross section of FEA model

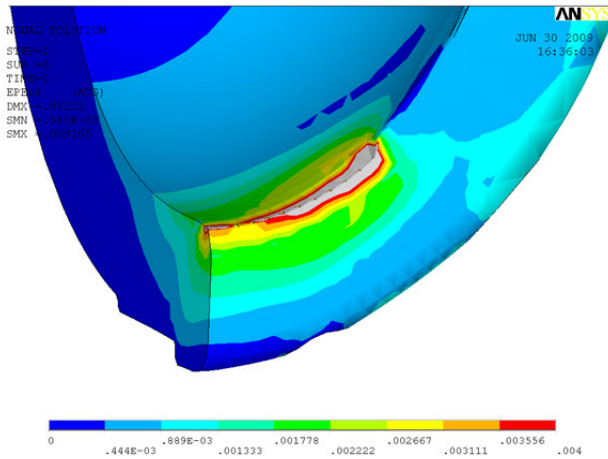


Figure 9: Maximum principle strain contours

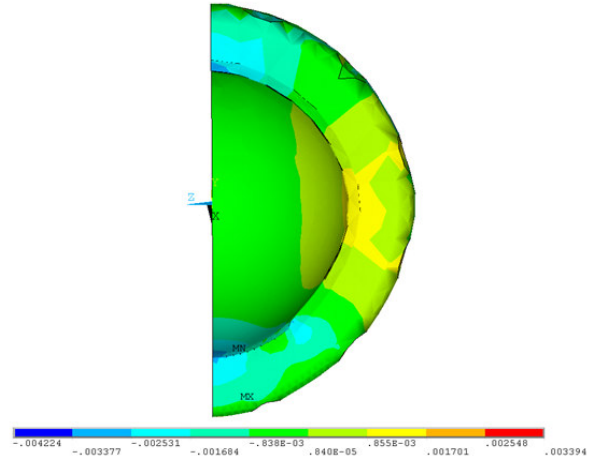


Figure 10: Strain in the z-direction (horizontal)

Finite element runs were made for 36 mm and 44 mm femoral heads with inclination angles of 45° and 65° and an offset of 2 mm. The resulting strain values corresponding to the direction associated with the fiber optic strain gages are summarized in Table 2. As seen in Table 2 the finite element models predict a larger strain in the thin liner than in the thick liner. One unusual result observed in the finite element models, and illustrated in Table 2, is that the thin liner was found to experience a tensile hoop strain, whereas the thick liner had a compressive hoop strain. In Table 2 the strain did not change significantly as a function of inclination angle. This is not to say that the total strain would not change, but rather that the strain that can be measured with the fiber optic strain gages did not change significantly.

Table 2: Finite element results for the strain in the direction and location of the fiber optic strain gages. The femoral head was offset 2 mm.

Head Size (mm)	Inclination (Degrees)	Inner Strain (%)	Middle Strain (%)	Outer Strain (%)
36	45	-0.211	N/A	-0.168
	65	-0.197		-0.197
44	45	N/A	0.433	N/A
	65		0.433	

4 Results

4.1 Specimen Testing

4.1.1 Tensile Test

The first set of tests performed after determining an appropriate adhesive was the tensile tests. A typical stress-strain curve obtained from the tensile test data is shown in Figure 11. The loading and unloading are included in this figure to show the hysteresis associated with this material. As seen in Figure 11, the results from the fiber optic and resistance strain gages correlated very well with the results from the extensometer. The stress-strain curve shown is clearly non-linear with no clear linear elastic region. This result was not unexpected, because X3 HCLPE is a viscoelastic material.

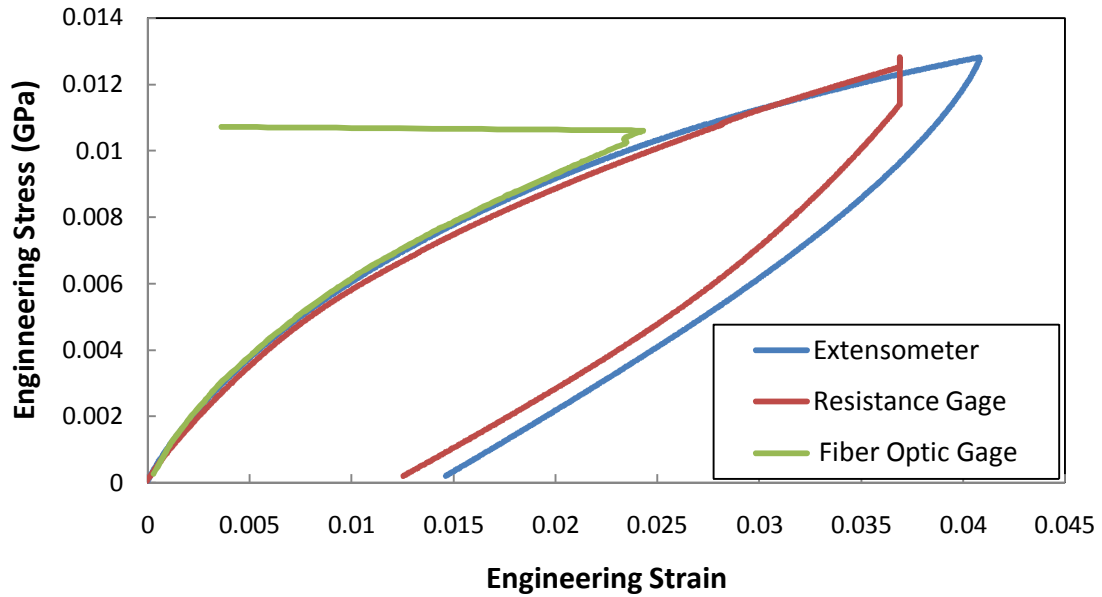


Figure 11: Typical tensile test result for X3 HCLPE

The long horizontal line associated with the fiber optic strain gage in Figure 11 corresponds to the point where the gage debonded from the sample. The fiber optic gages typically debonded at strains lower than the resistance gages. This is most likely due to the small contact area of the fiber for the epoxy in comparison to the resistance gage. Another peculiar feature in Figure 11 is the vertical line of strain associated with the resistance strain gage at about 3.75% strain. This occurred because the resistance strain measuring system became saturated at 10 V.

In Figure 12 is shown the extensometer results from all three tension tests. Clearly the extensometer results from the three tests were very consistent. The loads for tensile tests T1 and T2 were applied up to a strain of 4%, but for test T3 the load was inadvertently only applied up to a strain of 1%.

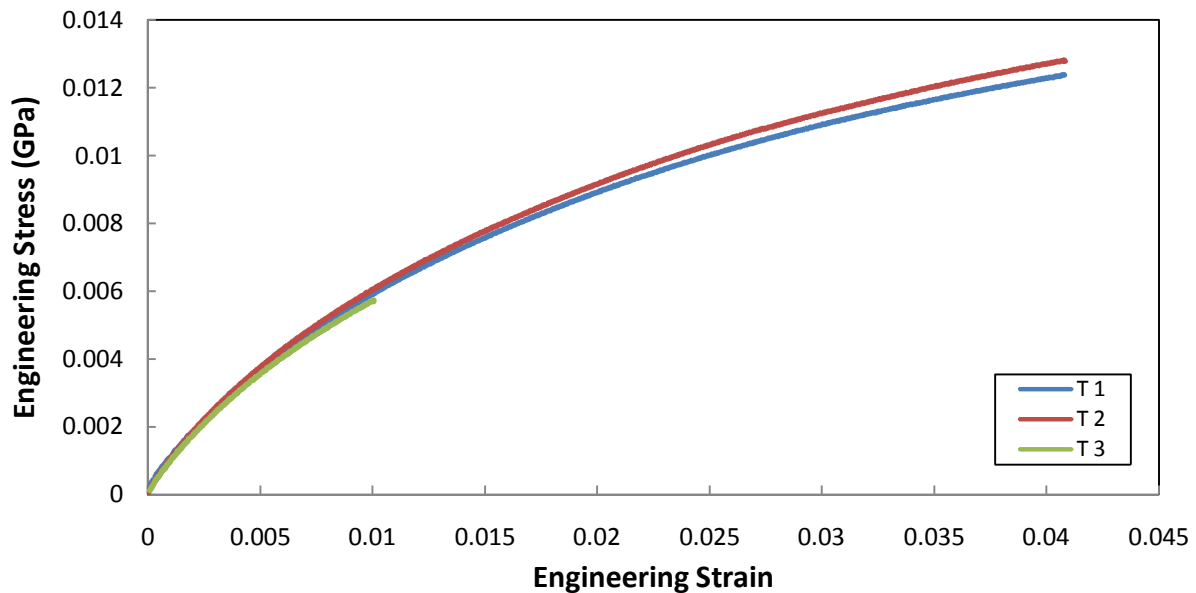


Figure 12: Tensile test results for X3 HCLPE found using the extensometer

The stress-strain curves found for the three tension tests using the resistance strain gages are shown in Figure 13. The resistance strain gage results were very consistent from one test to another. The results from test T1 and T2 only go up to about 3.5%, indicating that the system saturated before the 4% strain recorded by the extensometer.

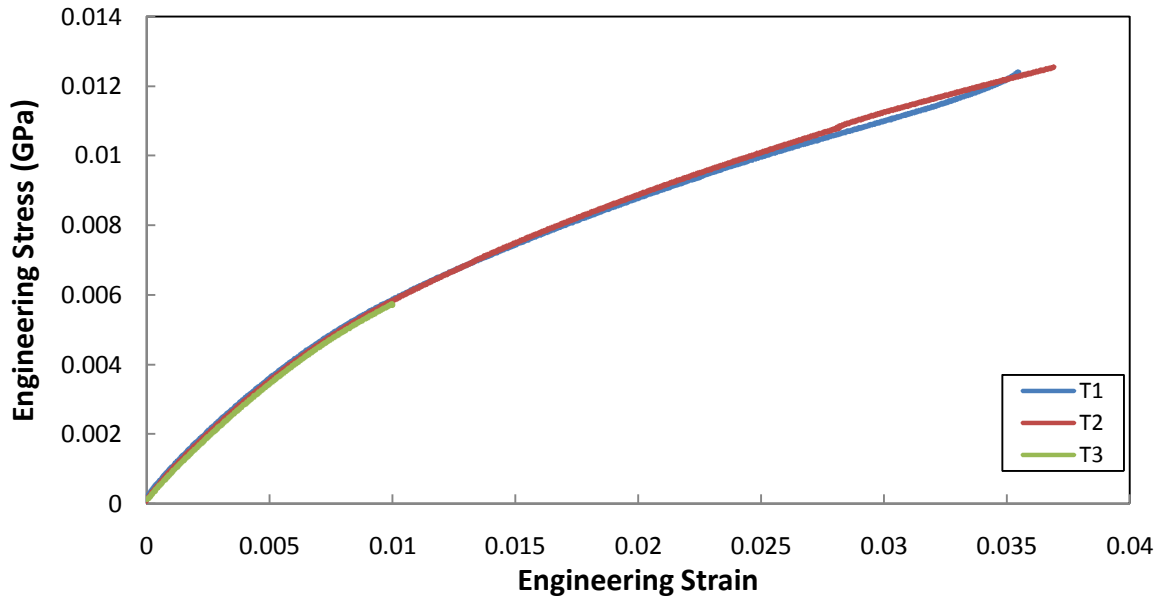


Figure 13: Tensile test results for X3 HCLPE found using resistance gages

The stress-strain curves found for the three tension tests using the fiber optic strain gages are shown in Figure 14. Once again the fiber optic gages gave consistent results from one test to another. The main difference between the fiber optic gage results and those from the other transducers is the maximum strain. For the fiber optic gages, the maximum strain is less than 2.5% because the bonds failed.

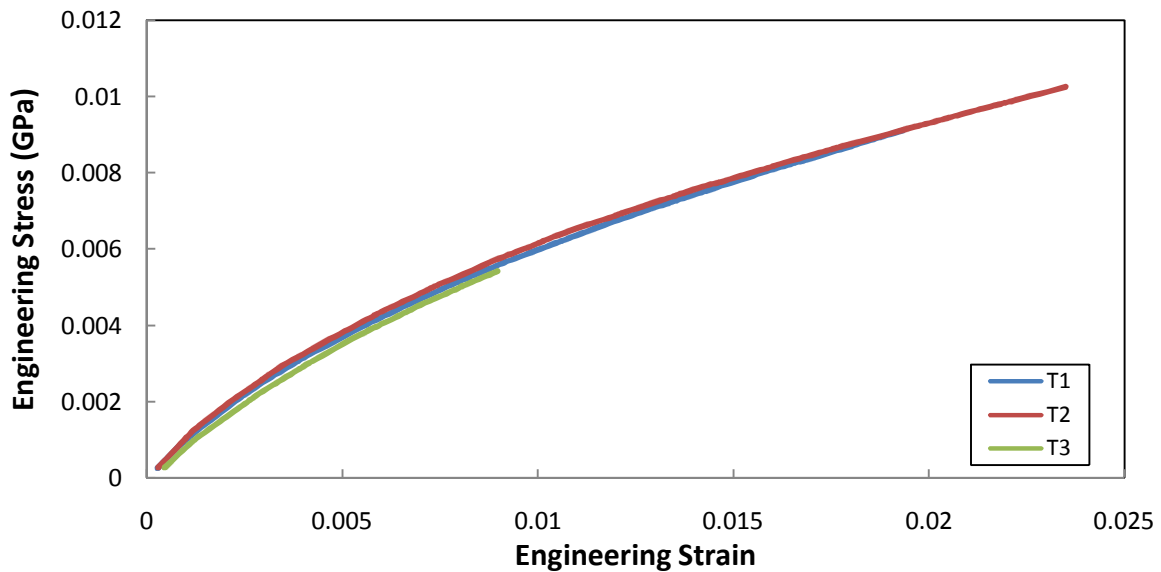


Figure 14: Tensile test results found for X3 HCLPE using fiber optic strain gages

Poisson's ratio was calculated at every value of strain using the lateral and the transverse resistance strain gages. The calculated value was then plotted against axial strain. Figure 15 shows a typical curve derived using this method. This plot shows the effects of dividing two very small numbers with experimental error during initial loading by the vertical asymptote near the origin. The curve then quickly levels out at $\nu = 0.408$.

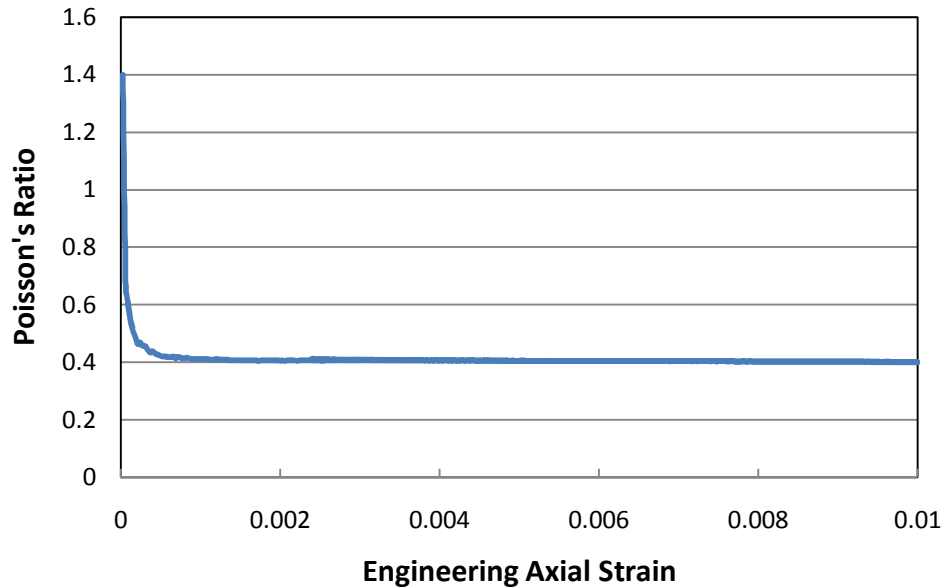


Figure 15: Poisson's ratio for X3 HCLPE calculated from test T3

The material properties determined from the tensile tests are shown in Table 3. The tangent modulus was calculated using the extensometer readings, and Poisson's ratio was calculated using the resistance gages for all three tests. The average tangent modulus calculated using the extensometer was 1.01 GPa. This value is slightly higher than non-cross-linked polyethylene, which has a tangent modulus of 0.830 GPa [5].

Table 3: Results from tension tests

Property	T1	T2	T3	Average
Elastic Modulus (GPa)	0.990	1.053	0.976	1.007
Poisson's Ratio	0.419	0.491	0.408	0.439

4.1.2 Compression Tests

After the axial tension tests were completed, compression tests of X3 HCLPE were performed. A typical stress-strain curve resulting from the compressive testing is shown in Figure 16. The compressive tests were only performed to a maximum strain of about 2%. In Figure 16 the vertical axis refers to the compressive stress. It is clear from Figure 16 that the results from the various transducers, that is, the fiber optic strain gage, resistance strain gage and extensometer did not correlate as well as they did for the tensile tests. The extensometer results and fiber optic strain gage results were fairly consistent, but the resistance strain gage reported a larger strain for a particular stress. This is most likely due to bonding issues associated with the epoxy. The results of various preliminary tests indicated that the results for the resistance strain gage and the fiber optic strain gage could vary significantly depending on the quality of the gage fixation, including the type of epoxy and the thickness of the epoxy layer. In the test shown in Figure 16, the gages differed by about 2 MPa at the peak strain.

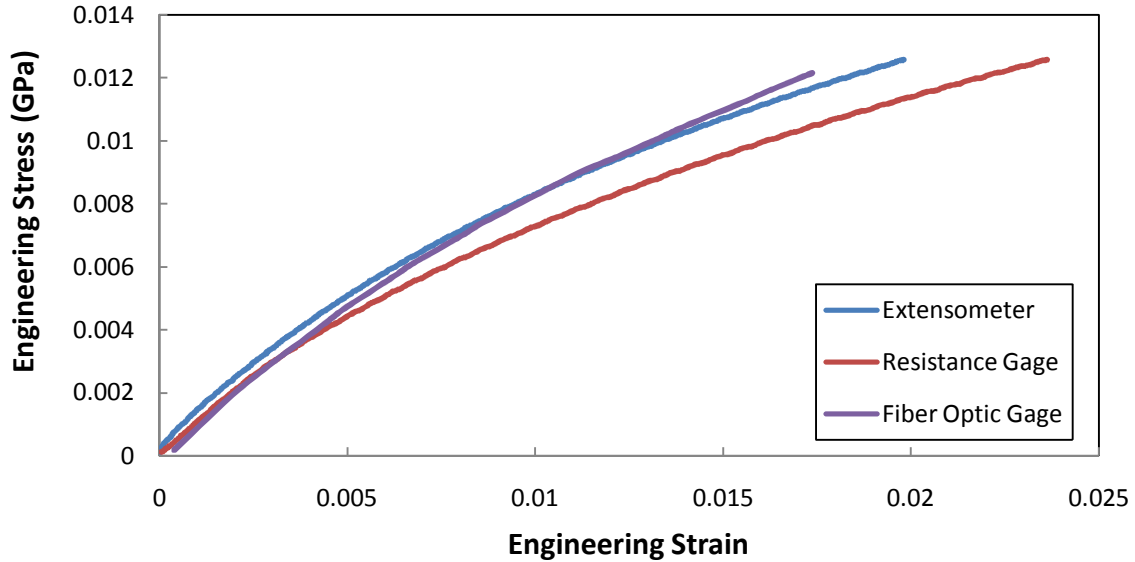


Figure 16: Typical compression curves for X3 HCLPE

Three samples were tested in compression and the stress-strain curves resulting from the extensometer data are shown in Figure 17. From this figure it is clear that the extensometer resulted in very consistent results from one test to another. The maximum percent difference between the extensometer results occurred at the maximum strain and was equal to only 0.20%.

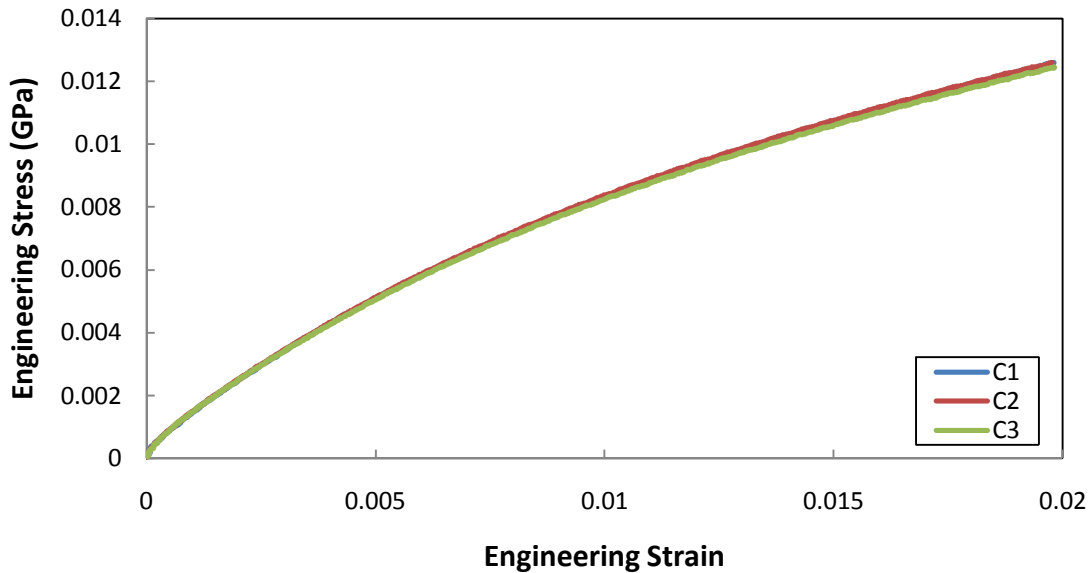


Figure 17: Compressive test results for X3 HCLPE found using the extensometer

Figure 18 shows the compression test results using the resistance strain gages. The resistance strain gage result from test C2 was found to deviate from the other tests quite drastically and in a non-linear fashion. After all the tests the samples were compared, and it was discovered that C2 had a thicker, non-uniform layer of epoxy which may explain the difference between this test and the others. The results from test C1 and C3 were consistent, but with a slight offset.

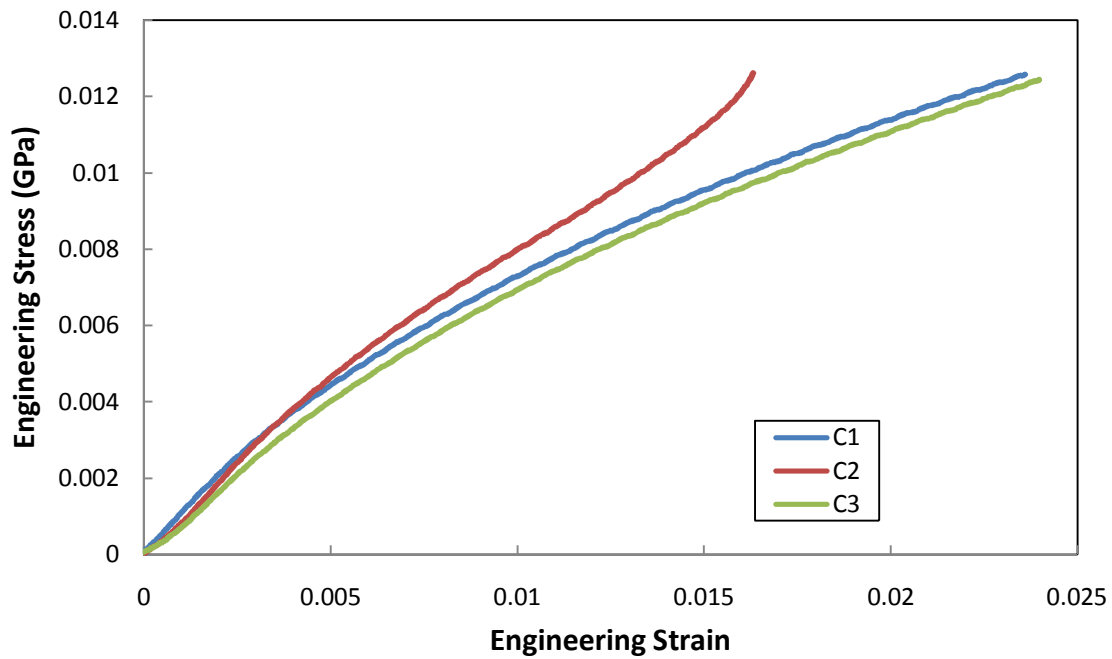


Figure 18: Compressive test results for X3 HCLPE found using resistive gages

Figure 19 shows the compression test results using the fiber optic strain gages. As seen in Figure 14 the results using the fiber optic strain gages were very consistent, although not as consistent as the extensometer result. Around 0.5% strain Test C3 showed an unusual jump in stress. The reason for this jump is not clear, although it may be due to the adhesive. The fiber optic gages for all three compression tests failed before the maximum strain recorded by the extensometer. These failures were likely due to the poor compressive strength of the epoxy and the small surface area for adhesion between the gage and the samples. The fiber optic gage that failed at the lowest strain was the one used for test C3, which debonded at about 1.1%.

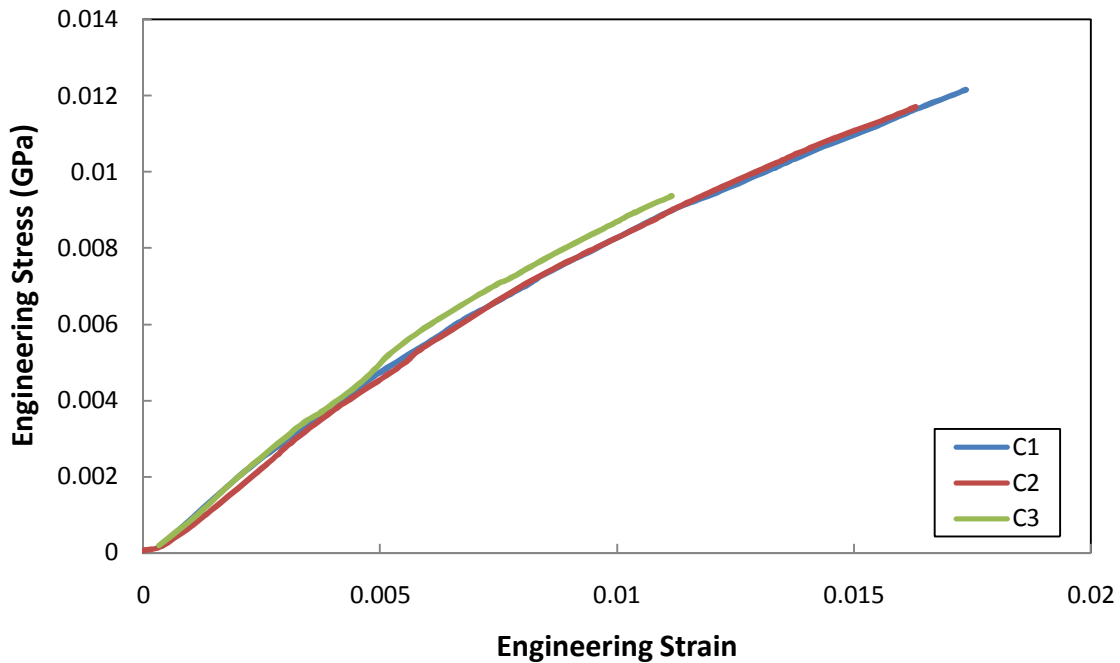


Figure 19: Compressive test results for X3 HCLPE found using fiber optic gages

Poisson's ratio for compression was plotted at all values of axial strain as shown for C2 in Figure 20. These results were determined using data from the transverse and longitudinal resistance strain gages. From this test a Poisson's ratio of about 0.4 was obtained. This compares favorably to the Poisson's ratio obtained from the tensile tests. The large deviation for small levels of strain is due to dividing two small numbers with experimental error. At about 1.4% strain the Poisson's ratio appears to rise slightly. This is different than the tensile test results, which diverged very little from the final value of Poisson's ratio. This trend may be due to a characteristic of the plastic when loaded in compression, but more data is necessary to determine if this trend continues.

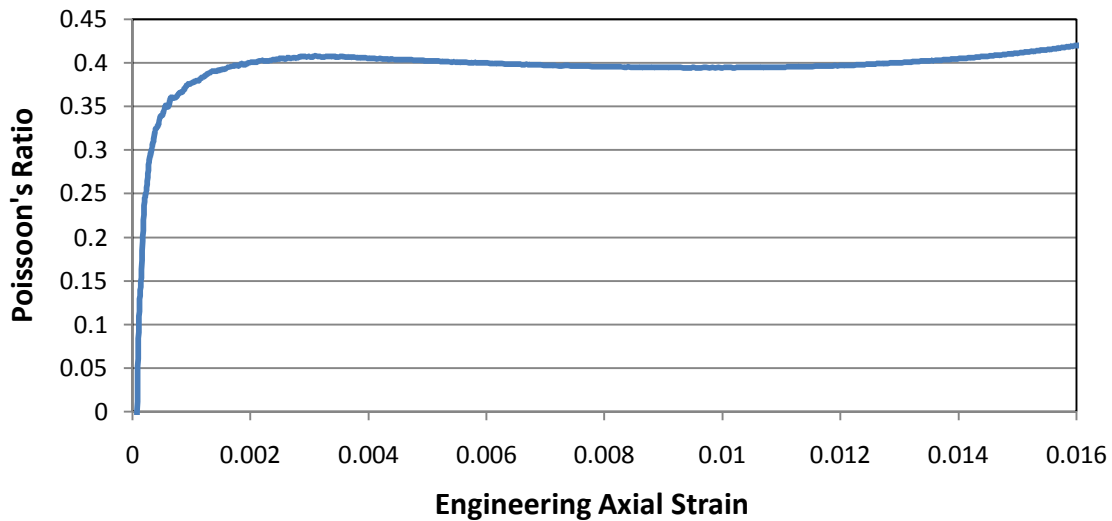


Figure 20: Poisson's ratio for X3 HCLPE calculated from test C2

The tangent modulus and Poisson's ratio obtained from the compression tests are summarized in Table 4. The tangent modulus was calculated using the extensometer data. In comparison with the average tangent modulus of 1.007 GPa for tension, the average tangent modulus for compression was 1.493 GPa.. The Poisson's ratios obtained for tension and compression were very similar with only a 5% difference between the two average values obtained.

Table 4: Results from the compression tests

Property	C1	C2	C3	Average
Tangent Modulus (Gpa)	1.428	1.518	1.534	1.493
Poisson's Ratio	0.399	0.406	0.453	0.419

4.2 Clinical Testing

After the tension and compression tests were completed, the tests simulating clinical loading were performed. In Figure 21 are shown the hoop strains obtained from the fiber optic strain gages closest to the load for the tests on the 36 mm diameter X3 HCLPE liners. As can be seen in this figure, the strain was found to generally increase as the offset increased for all inclination angles. As expected, the tests at 45° showed lower strain measurements than the tests at 65°. However, the tests at 55° showed lower strain than both of the other tests, at least at the strain gage location. Recall that only the hoop strain is being measured and not the total strain.

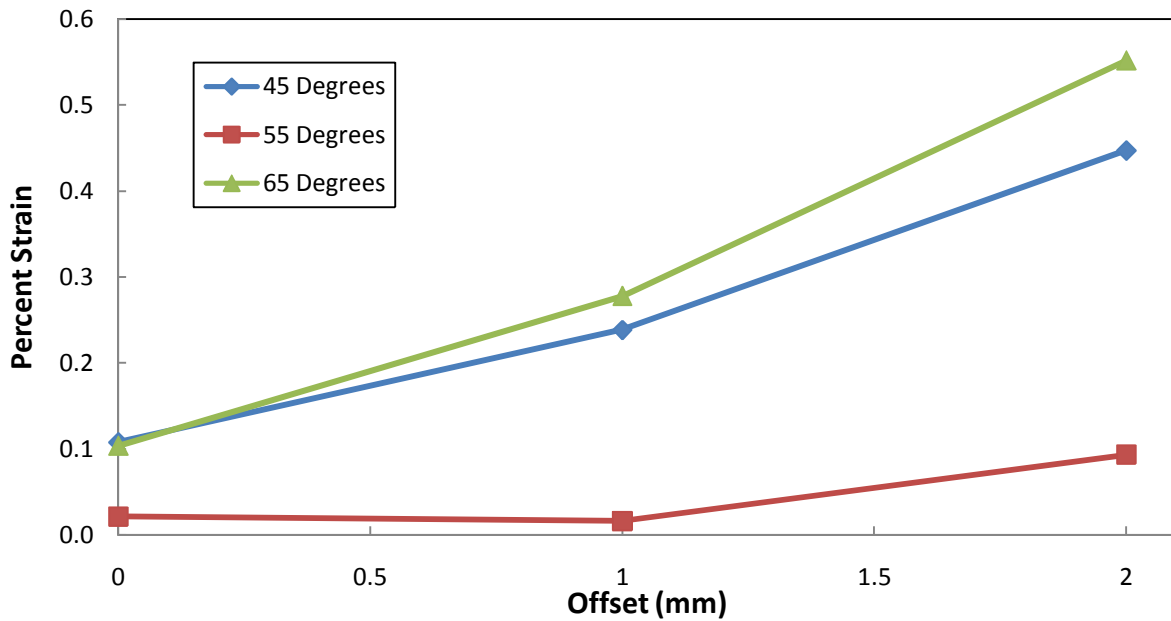


Figure 21: Hoop strain obtained from the strain gages closest to the load for the tests on the 36 mm diameter X3 HCLPE liners.

Table 5 shows the numerical values for the 36 mm diameter liner results as shown in Figure 21. This table shows the percent strain as measured by the fiber optic gages for all parameter variations. The inner strain is the strain measured by the fiber optic gage that was closest to the load application. The outer strain is the strain measured by the fiber optic farthest from the load application. From this table it is clear that the hoop strain was smaller for the strain gages located farther from where the load was applied. The outer strain measurements on the 36 mm liner were quite small and showed no clear trend. This is most likely due to the fact that the strains at that point were too small to measure accurately. In Table 5 are also shown the results from the finite element analysis. Clearly, there was a significant difference between the analysis results and the testing results which requires further investigation.

Table 5: Results from 36 mm diameter X3 liner

Liner Diameter (mm)	Material	Load Angle (deg)	Offset (mm)	Experimental		FEA Analysis	
				Inner Strain (%)	Outer Strain (%)	Inner Strain (%)	Outer Strain (%)
36	X3	45	0	0.1080	-0.0004		
			1	0.2387	0.0025		
			2	0.4474	0.0017	-0.2110	-0.1680
		55	0	0.0211	-0.0004		
			1	0.0161	0.0000		
			2	0.0934	-0.0079		
		65	0	0.1038	-0.0062		
			1	0.2778	0.0000		
			2	0.5518	0.0012	-0.1970	-0.1970

Figure 22 displays the clinical testing hoop strain results for the 40 mm diameter liner. As seen with the 36 mm diameter liner, the trends for the inner strain values are relatively consistent while the outer measurements are not. It can be seen that the strain transitions from compressive to tensile after the offset is increased to 2 mm for every test except for the data acquired from the 65° 1 mm offset. Also, except for the strain recorded at the 65° angle with a 2 mm offset, the strains increase with increasing angle.

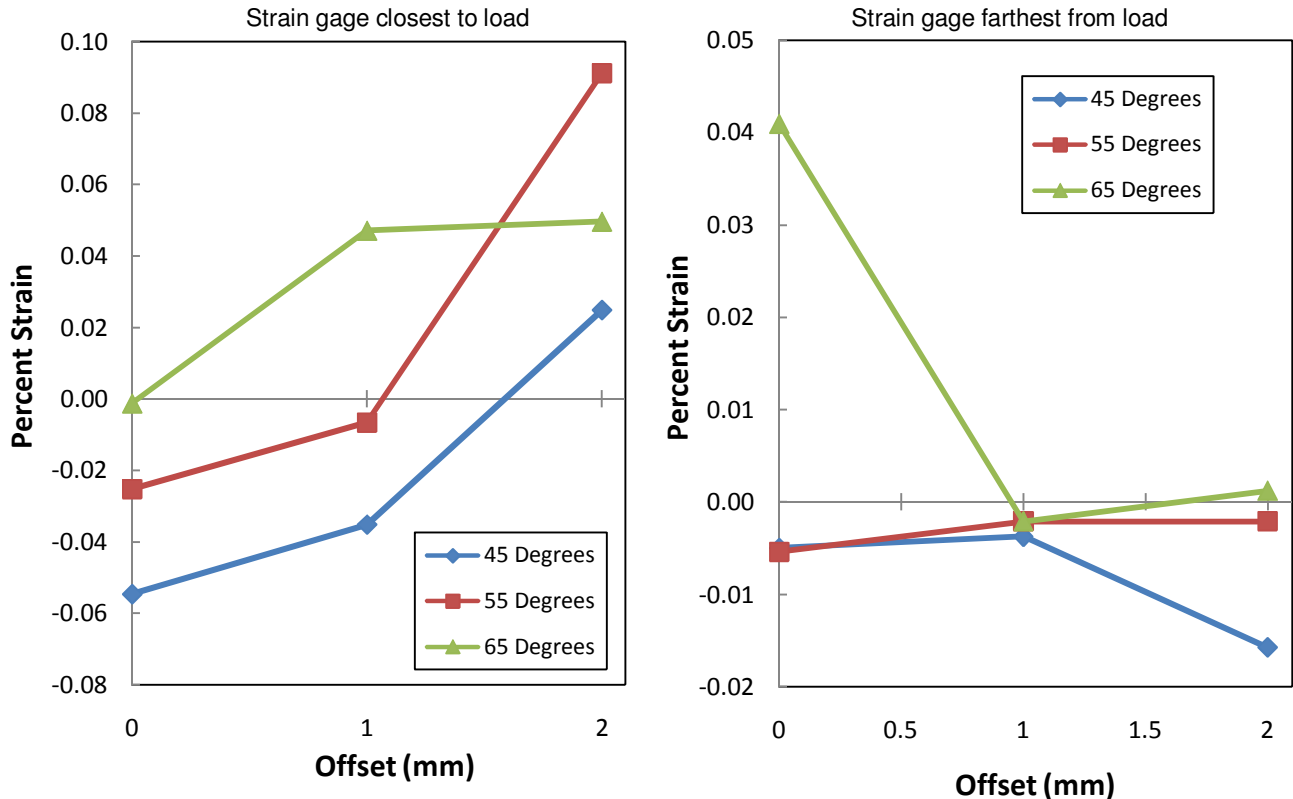


Figure 22: Hoop strain obtained from the strain gages for the tests on the 40 mm diameter X3 HCLPE liners.

Figure 23 shows the clinical testing results for the 44 mm diameter liners made from N2Vac and X3 HCLPE. This size liner was the thinnest liner tested and had one fiber optic gage in the middle of the lip of the liner. Increasing the offset of the load did not create a trend in the strain values. The values of strain for the liner made from X3 HCLPE fluctuated between -0.02 and -0.07 percent strain for all loading situations except 65° with 2 mm offset where there was a significant increase in the strain. The results for the 44 mm diameter head results using the N2Vac material showed an increasing strain with increasing angle. Additionally, as with the 44 mm head made of X3 HCLPE, there is a general compressive to tensile change as offset is increased for each angle group. For a 65° angle the strain in the X3 HCLPE liner was higher than the strain in the N2Vac liner for every offset. For the 45° and 55° angles offset this was not the case – sometimes the strain in the X3 liner was higher and sometimes it was lower.

Finite element results were available for only two of the test configurations. These results are shown in Table 6. The FEA results for the 45° loading angle with 2 mm offset were tensile, however the experimentally found values were compressive. However, the FEA results and experimental data for the 65° loading angle with 2 mm offset were both tensile, although the numerical values were quite different. The strain found through the numeric model was much larger than the strain determined experimentally.

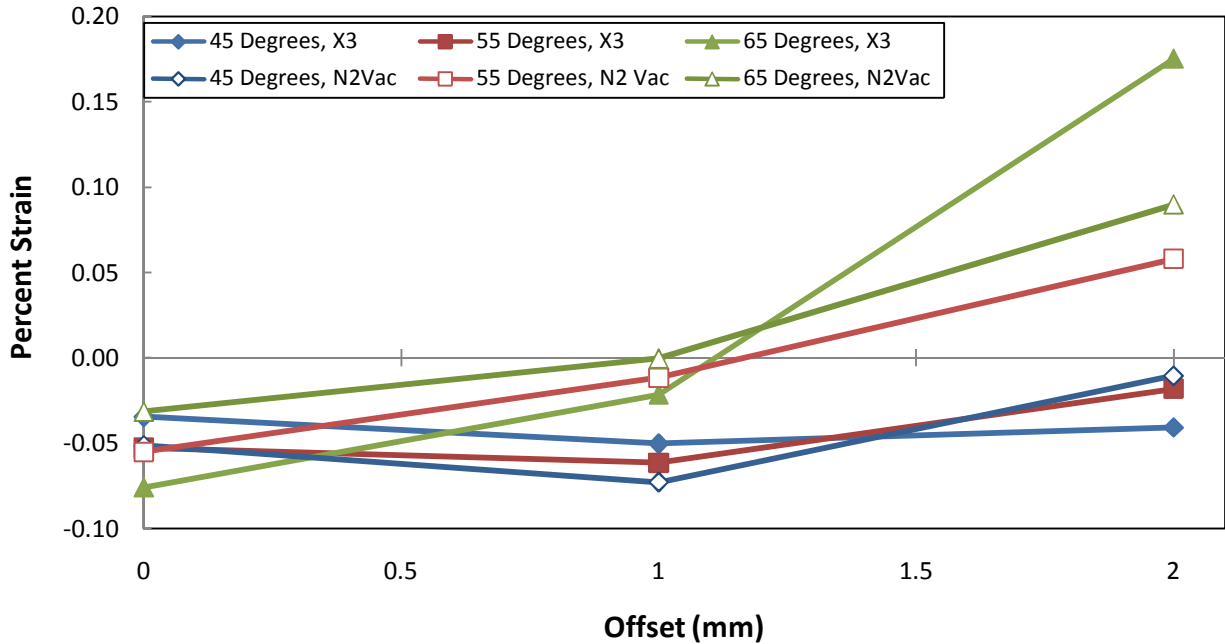


Figure 23: Results from 44 mm diameter N2Vac and X3 HCLPE liners

Figure 6: Comparison of finite element results and experimental results for the 44 mm liner made from X3

Load Angle (deg)	Offset (mm)	Experimental	FEA Analysis
		Middle Strain (%)	Middle Strain (%)
45	2	-0.0406	0.4330
65	2	0.1751	0.4330

From the above tables and analysis, it is clear that the finite element results did not agree with the experimental results. Because the fiber optic gages were shown to produce good data in tension and compression during the material testing, it is believed that the material models used for the finite element analysis should be improved.

5 Conclusions and Recommendations

In this study, standard tension and compression samples of X3 HCLPE were tested and hip liners subjected to realistic loadings were tested for various inclination angles and offsets. Bonding the strain gages to X3 HCLPE proved to be more difficult than anticipated. This was primarily due to the material's low surface tension and the adhesive's inadequate wetting. Bondit was found to provide a relatively good bond between each type of gage and the polyethylene, although in every failure of a fiber optic gage the adhesive failed before the fiber itself. Another problem experienced with the fiber optic strain gages was that they were very delicate and broke easily while being installed.

The tension tests showed that the stress-strain curves obtained using data from the fiber optic strain gages and the resistance strain gages agreed well with results found using the data from the extensometer. For tension, the average tangent modulus calculated using the extensometer was about 1 GPa which was slightly higher than non-cross-linked polyethylene. In the compression tests there was more variability between the fiber optic strain gage, resistance strain gage, and extensometer results. The extensometer had the best correlation from one test to another. The variability in the other tests is most likely due to bonding issues with the epoxy. For compression, the average tangent modulus calculated using the extensometer was about 1.5 GPa and a Poisson's ratio of about 0.4 was obtained in both the tension and compression tests.

The results obtained from hip liners of various thickness indicated relatively small hoop strains in all cases. The shell for the 35 mm head had the largest measured hoop strains, which could be due to the choice of locations for the gages. Unfortunately, it was not possible to measure the transverse shear, so no observations can be made concerning the total strain as a function of thickness. The results from the finite element model did not correlate well with the experimental results.

References

- [1] Frey, R. *Encyclopedia of Surgery: A Guide for Patients and Caregivers*. surgeryencyclopedia.com. [Online] Advameg, Inc., 2007. [Cited: 07 23, 2009.]
- [2] Crownshield, R., W. Maloney, D. Wentz, S. Humphrey, C. Blanchard. *Bio Mechanics of Large Femoral Heads, What They Do and Don't Do*. Clinical Orthopaedics and Related Research. 2004; 429:102-107.
- [3] Lombardi, A., T. Mallory, D. Dennis, R. Komistek, R. Fada, E. Northcut. *An in vivo determination of total hip arthroplasty pistoning during activity*. The Journal of Arthroplasty. 2000;15(6):702-709
- [4] Paul, J.P. *Approaches to design: Force actions transmitted by joints in the human body*. Proc. R. Soc. Lond. B. 1976;192:163-172
- [5] Kurtz, S., *Ultra High Molecular Weight Polyethylene in Total Joint Replacement*, The UHMWPE Handbook, 2002;263
- [6] Yau, Shi-Shen. Shi-Shen.Yau@stryker.com. Request for information on X3 and N2Vac. 19th August 2009.
- [7] Stryker. *X3 Sequentially Annealed Irradiated Polyethylene*. X3 The power of Technology. (Technical data sheet) 2006.
- [8] Kersey, A. D., M. A. Davis, H. J. Patrick, M. LeBlanc, K. P. Koo, C.B. Askins, M. A. Putnam, and E. J. Friebele, *Fiber grating sensors*, J. Lightwave Technology. 1997;15:1442-1463
- [9] Todd, M., D. Inman, *Optical-Based Sensing*, in Damage Prognosis, John Wiley and Sons Inc. (Chichester, UK) 2004.
- [10] Lopez-Higuera J.M., *Handbook of Optical Fiber Sensing Technology*, John Wiley and Sons, Inc. (Chichester, UK), 2002.
- [11] Udd E, *Fiber Optic Sensors: An Introduction for Scientists and Engineers*, Wiley Interscience, 2006.
- [12] Limited, Roctest. Rocktest USA. [Online] 2004. [Cited: July 27, 2009.] http://www.roctest.com/modules/AxialRealisation/img_repository/files/documents/FOS.pdf.

- [13] Rao M, Bhatt M.R., Murthy C.R.L., Madhav K, Asokan S. *Structural Health Monitoring Using Strain Gages, PVDF Film and Fiber Bragg Grating Sensors: A Comparative Study*. Proc. National Seminar on Non-Destructive Evaluation, 2006:333-337
- [14] Fourche G, An Overview of the Basic Aspects of Polymer Adhesion. Part 1: Fundamentals. *Polymer Engineering and Science*. 1995;35(12):957-967
- [15] Briassoulis D, Schettini E. *Measuring strains of LDPE films: the strain gage problems*, *Polymer Testing* 21. 2002;507-512
- [16] D695-08, Standard Test Method for Compressive Properties of Rigid Plastics
- [17] D638-08 Standard Test Method for Tensile Properties of Plastics